Supplementary Information

Comparison of electronic resistance measurement methods and influencing parameters for LMFP and high-nickel NCM cathodes

Christoph Seidl[1,2,*], Sören Thieme[1], Martin Frey[1], Kristian Nikolowski[3], Alexander Michaelis[2,3]

[1] Mercedes-Benz AG, Mercedesstraße 120, 70327 Stuttgart, Germany;
[2] Institute of Materials Science, TU Dresden, 01062 Dresden, Germany
[3] Fraunhofer IKTS, Fraunhofer Institute for Ceramic Technologies and Systems, 01277 Dresden, Germany
* corresponding author: christoph.seidl@mercedes-benz.com

S1. Hsu and Mansfeld formula Formula

Formula commonly used to convert CPE data to double layer capacities [1,2]:

$$C = \left(\frac{Q}{R^{\alpha-1}}\right)^{\frac{1}{\alpha}} \quad \text{(S1)}$$

C… Capacitance / C
Q… CPE coefficient / Ω s-α
α… Exponent / 1
R… Resistance of resistor parallel to CPE / Ω

S2. 46-point probe measurement

Figure S1 shows pictures of the 46-point probe measurement device (HIOKI RM2610) to facilitate better understanding of the measurement procedure and principle.

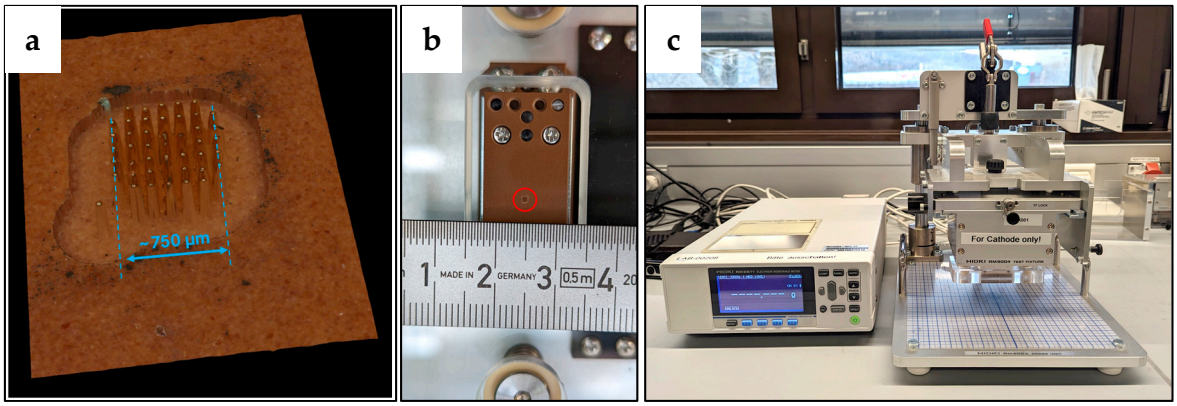

Figure S1. (a) 3D microscopy picture of the measurement pins. (b) Picture of the measurement head. (c) Picture of the HIOKI RM2610 measurement system.

Figure S2 shows a schematic of the measurement principle of the 46-point probe method (HIOKI RM2610). Which should facilitate better understanding with the description in section 2.3 in the main paper.

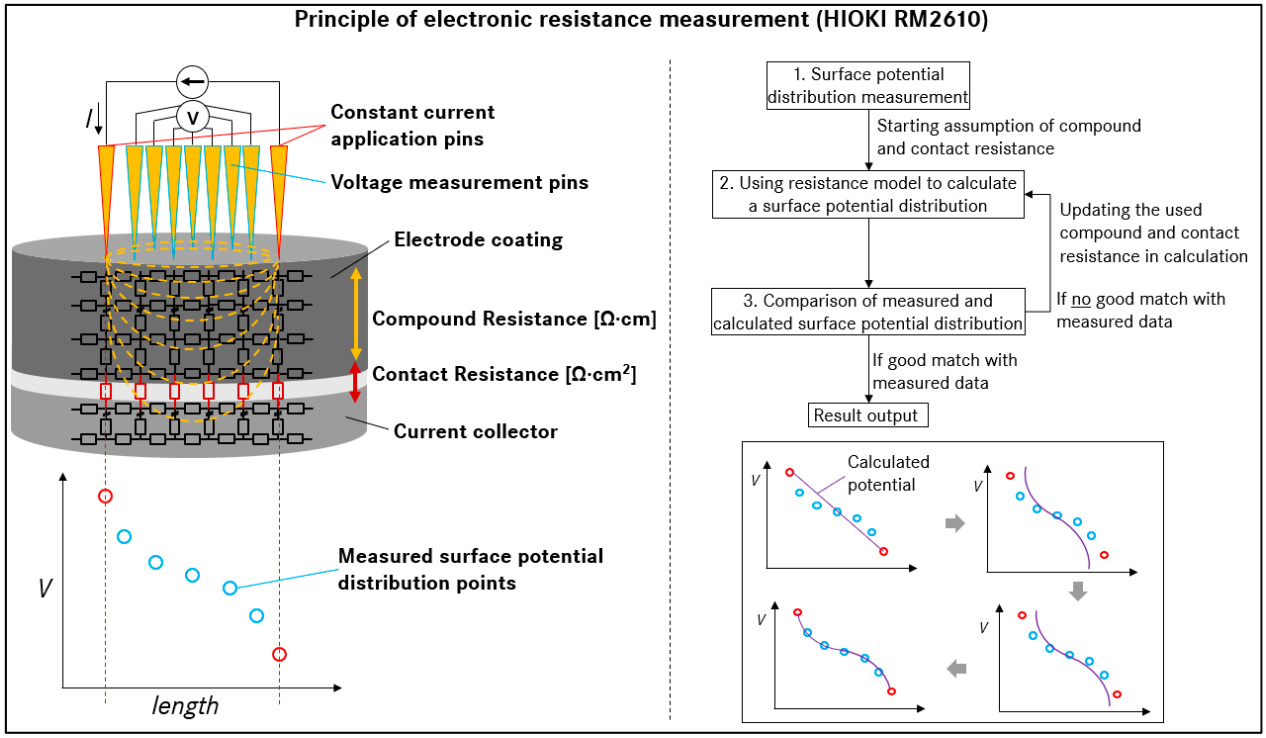

Figure S2. Schematic of the measurement principle of the 46-poin probe method (HIOKI RM2610). Adapted with friendly permission from [3].

S3. 2-point measurement scheme

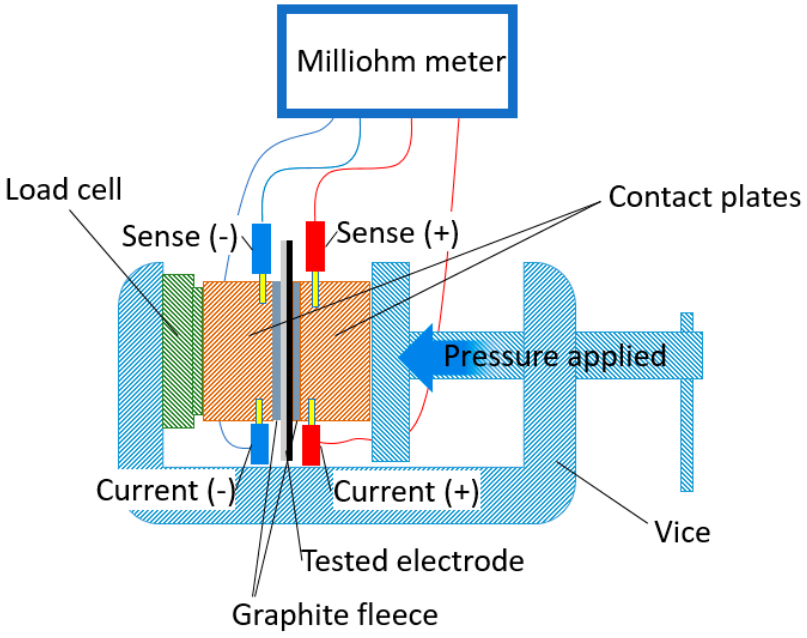

Figure S3. Scheme of the measurement setup used for 2-point measurements. Further details explained in experimental section of main paper.

S4. Detailed description of equivalent circuit model (ECM)

A constant-phase-element (CPE) is used to account for low frequency diffusion effects, which can originate from solid-state-diffusion of Li^+ in the active material or the electrolyte diffusion in the separator [4]. A serial Ohmic resistance (R_{Serial}) accounts for typical Ohmic resistance responses such as resistance of electrolyte (usually largest part of R_{Serial}) and electronic resistances of the current collectors and wiring. A CPE in parallel with an Ohmic resistance (CPE-R element) describes the charge-transfer (R_{ct}) of Li^+ from electrolyte into the active material particle. Resistances along the transmission line on the electrolyte side describe the ionic resistance (R_{Ion}) within the pores of the electrode.

The ionic resistance of the electrolyte in free space or in separator (herein part of R_{Serial}) is consisting of the "migratory" resistance of ionic electrolytes in an electric field. This type of resistance has an intrinsically fast response time, meaning it occurs at very high frequencies or in most studies in the R_{Serial} part of an impedance spectra [5]. The ionic resistance in the electrode (herein R_{Ion}) occurs at lower frequencies than the migratory response of electrolyte in R_{Serial}. This is due to the build-up of double layers and voltage drop along the porous structure of an electrode. The effect can also be interpreted as a transport of ions along the depth of the pores. As the charge transfer occurs along the pores, the typical EIS response (45° slope) emerges [6].

Another set of resistances along the transmission line of the compound describe the electronic resistance of the electrode compound ($R_{Compound}$). Another CPE-R element outside of the transmission line is assumed to account for the electronic resistance between the electrode compound and the current collector ($R_{Contact}$).

$R_{Compound}$ can not be directly determined with EIS as it is overlaying with the serial resistance (R_{Serial}). In various studies $R_{Compound}$ is assumed to be much smaller than R_{Ion} and is therefore shortened [7]. Another possible solution is to fix the parameter at a measured value, which was done in this study. The $R_{Compound}$ was fixed at the value measured with the 46-point probe method. The $R_{Compound}$ is commonly considered to be very low in comparison to other contributions in the EIS spectra [7] and its proportion to $R_{Contact}$ is further discussed in section 3.3 of the main paper.

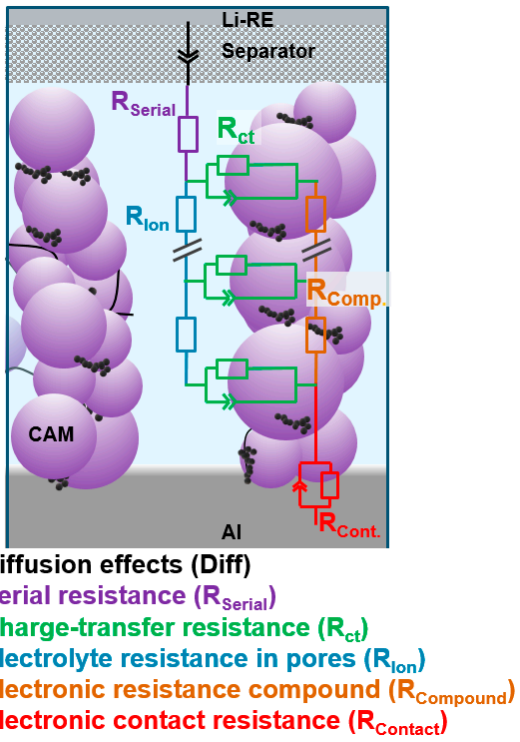

Figure S4. Scheme of the transmission line model based equivalent circuit used for impedance measurement fittings in this work

S5. $ASR_{Contact}$ of LMFP in Fe^{2+}/Fe^{3+} and Mn^{2+}/Mn^{3+} region

As it can be seen in Figure 2 of the main paper, the $R_{Contact}$ of the Fe^{2+}/Fe^{3+} redox region is slightly higher compared to the $R_{Contact}$ of the Mn^{2+}/Mn^{3+} redox region.

In between, there is a stepwise resistance decrease around 25-30 % SoC, once again associated with the change of redox regions. It is rational to assume that this behavior is caused by a change in electronic conductivity of the LMFP particle due to transition between less conductive $Li_xMn_{0.7}Fe_{0.3}PO_4$ ($x > 0.7$) and more conductive $Li_xMn_{0.7}Fe_{0.3}PO_4$ ($x < 0.7$) phases at this point. Another potential reason could be an increase of contact area between compound and current collector. The latter explanation, however, seems less probable since LMFP actually shrinks upon lithium extraction, which would cause a reduction in contact area at higher SoC (=lower state of lithiation).

S6. Comparison of resistance from pulse (GITT) vs. EIS

In Figure S5 the resistance of the cathode was calculated and compared by use of two different methods. The black squares indicate the resistance yielded by fitting of the EIS spectra and adding up the contribution of R_{ct} and $R_{Contact}$. The red dots are resistances calculated by using the pulse response of the cathode. The full voltage plot can be seen in the main paper Figure 2 (b). The resistance was calculated by using the voltage difference between the peak of the pulse and the voltage after one second of relaxation. Interestingly it can be seen that the two resistance values generally match very well. However, in the region of around 30% SoC the resistance in EIS shows a much stronger increase than the resistance from pulse. This behavior may be caused by the impact of solid-state diffusion in the resistance. Solid state diffusion may have a more important part in the total resistance measured in EIS. In the pulse this resistance is partly omitted because just the first second after pulse was used for evaluation. The same argumentation holds true for the differences in the higher SoC area.

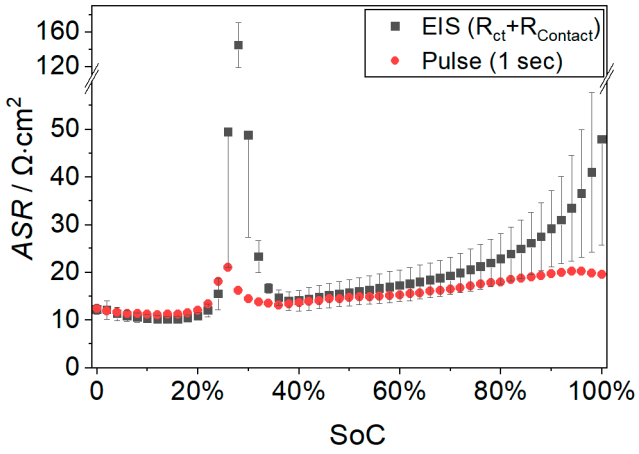

Figure S5. Areal specific resistance values from cathode in 3-electrode measurement calculated by EIS and current pulse.

S7. EIS Measurements of LMFP cathodes

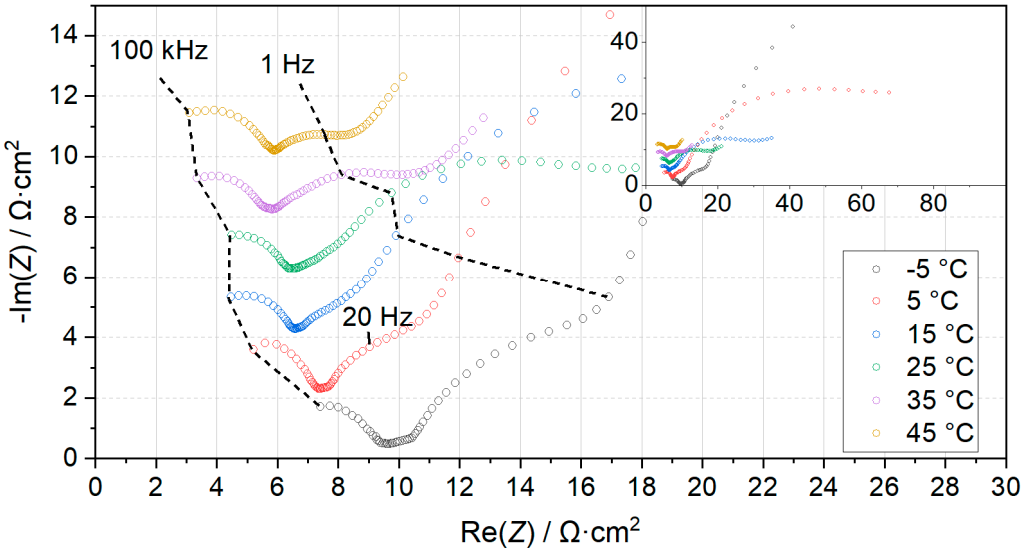

Figure S6. EIS spectra of calendered LMFP cathode (porosity: 50 %) coated on aluminum current collector (Al-CC) measured at 50 % SoC at various temperatures. In the 5 °C measurement the apex of an additional semicircle (20 Hz) is indicated.

Table S1. RSerial values from fitting of impedance spectra shown in Figure S6at SoC of 50 % at all temperatures measured.

Temperature / °C	**R_{Serial} value from fitting / Ω·cm²**
-5	4.06
5	3.12
15	3.03
25	2.57
35	1.91
45	1.51

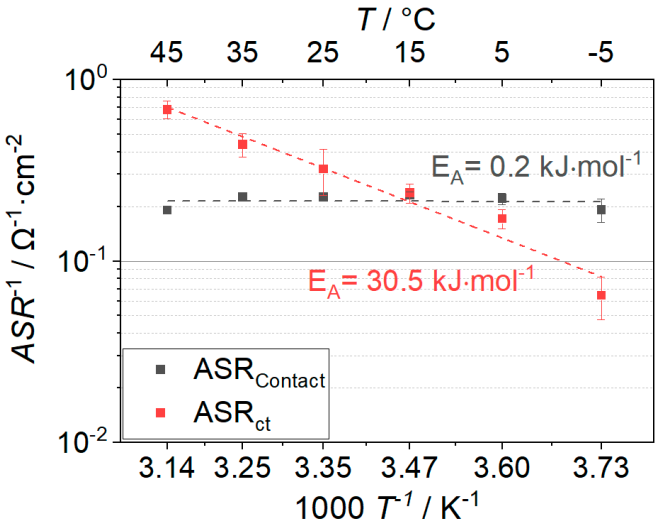

Figure S7. Arrhenius plots of both $ASR_{Contact}$ and ASR_{ct} calculated from EIS measurements of LMFP cathodes on Al-CC at 10 % SoC at various temperatures. The activation energy values were determined by linear data fitting. Error bars indicate the standard deviation of three cells. $R_{Contact}$ becomes a larger resistance contribution than R_{ct} already at 15 °C. At all higher temperatures $R_{Contact}$ is larger than R_{ct}.

S8. Influence of loading on electronic resistance of cathodes

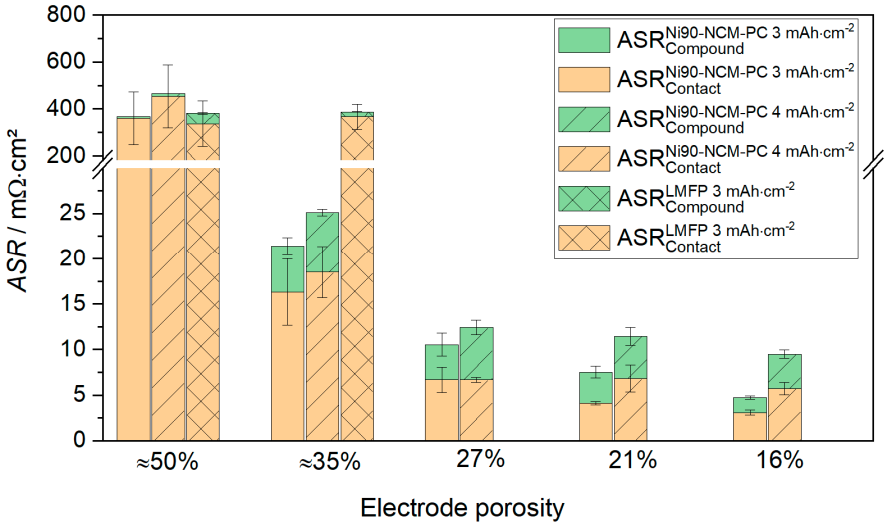

Figure S8. Electronic resistances measured with 46-point probe for a Ni90% NCM cathode with poly crystal structure (Ni90-NCM-PC) with loadings of 3 mAh cm-2 and 4 mAh cm-2. Values for LMFP cathode are shown for comparison reasons.

S9. Adhesion test for cathodes

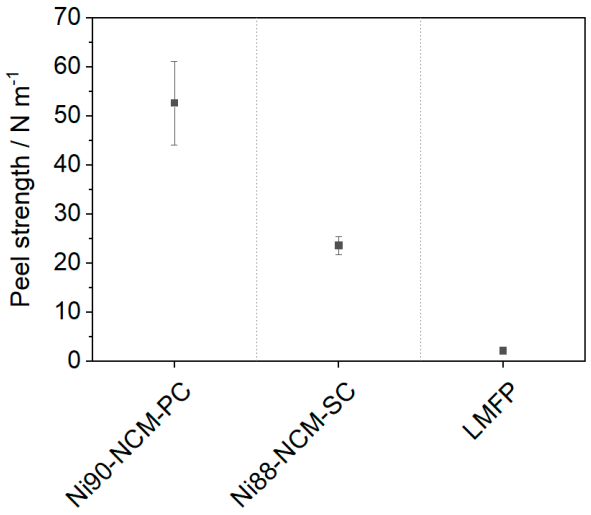

Figure S9. Peel strength of different tested electrode coatings applied on aluminum current collector. All electrodes had a loading of 3 mAh cm^{-2}. NCM cathodes had a porosity of 27 %, whereas LMFP cathode had a porosity of 35 %. The NCM materials include Ni90% poly crystal type (Ni90-NCM-PC) as well as Ni88% single crystal type (Ni88-NCM-SC). Adhesion data was measured with

a 90° peel test method. Here the mean values and standard deviation are plotted acquired from four measurements per electrode.

References

1. Hsu, C.; Mansfeld, F. Technical Note: Concerning the Conversion of the Constant Phase Element Parameter Y0 into a Capacitance. *Corrosion* **2001**, 747–748.
2. Hirschorn, B.; Orazem, M.E.; Tribollet, B.; Vivier, V.; Frateur, I.; Musiani, M. Determination of effective capacitance and film thickness from constant-phase-element parameters. *Electrochimica Acta* **2010**, *55*, 6218–6227, doi:10.1016/j.electacta.2009.10.065.
3. HIOKI E.E. CORPORATION. RM2610 Electrode Resistance Measurement System Instruction Manual. Available online: https://www.hioki.com/euro-en/products/resistance-meters/resistance/id_6740 (accessed on 5 March 2024).
4. Heubner, C.; Nikolowski, K.; Reuber, S.; Schneider, M.; Wolter, M.; Michaelis, A. Recent Insights into Rate Performance Limitations of Li-ion Batteries. *Batteries & Supercaps* **2020**, doi:10.1002/batt.202000227.
5. Newman, J.; Thomas-Alyea, K.E. *Electrochemical Systems*, 3rd Edition; Wiley & Sons Ltd: Hoboken, NJ, USA, 2012; ISBN 0-471-47756-7.
6. Moškon, J.; Gaberšček, M. Transmission line models for evaluation of impedance response of insertion battery electrodes and cells. *Journal of Power Sources Advances* **2021**, *7*, 100047, doi:10.1016/j.powera.2021.100047.
7. Landesfeind, J.; Ebner, M.; Eldiven, A.; Wood, V.; Gasteiger, H.A. Tortuosity of Battery Electrodes: Validation of Impedance-Derived Values and Critical Comparison with 3D Tomography. *J. Electrochem. Soc.* **2018**, *165*, A469-A476, doi:10.1149/2.0231803jes.